John von Neumann Institute for Computing

Double Black Holes in Galactic Nuclei – Do they Merge or not?

Marc Hemsendorf, Rainer Spurzem, Steinn Sigurdsson

published in

NIC Symposium 2001, Proceedings,
Horst Rollnik, Dietrich Wolf (Editor),
John von Neumann Institute for Computing, Jülich,
NIC Series, Vol. **9**, ISBN 3-00-009055-X, pp. 51-60, 2002.

http://www.fz-juelich.de/nic-series/volume9

Double Black Holes in Galactic Nuclei – Do they Merge or not?

Marc Hemsendorf[1,2], **Rainer Spurzem**[2], **and Steinn Sigurdsson**[3]

[1] Department of Physics & Astronomy
Rutgers University, 136 Frelinghuysen, Piscataway N.J. 08854-8019 U.S.A.
E-mail: marchems@physics.rutgers.edu

[2] Astronomisches Rechen-Institut, Mönchhofstrasse 12-14, 69120 Heidelberg, Germany
E-mail: spurzem@ari.uni-heidelberg.de

[3] Department of Astronomy & Astrophysics, 525 Davey Lab.
Penn State University, University Park PA 16802 U.S.A.
E-mail: steinn@najma.astro.psu.edu

We investigate with high accuracy direct numerical N-body integrations the time-evolution of dense stellar systems harboring a massive black hole. This is a model for galactic nuclei in centres of galaxies after they merge in the context of cosmological galaxy formation and evolution. An important astrophysical question is how fast these black holes come close to each other due to dynamical friction and superelastic scatterings with field stars. At a certain critical separation they would spiral-in and merge induced by gravitational radiation. The computer programmes *EUROSTAR* and *NBODY6++* developped for use with mpi libraries maintain high accuracy over billions of integration timesteps, allowing a detailed analysis of the orbit of the black hole(s), its interactions with field stars, and the two-body relaxation in the surrounding dense stellar system.

1 Binary Black Holes in Galactic Nuclei

Massive black holes are very likely to reside in the centres of galaxies as a fossile of earlier acticity[16,18]. For their formation collisionless dynamical general relativistic collapse or dissipative processes during galaxy formation have been proposed[32], but a complete and quantitative understanding does not yet exist (compare, however, some related work in that direction in[17,4]). Nowadays there is strong evidence that the formation of central black holes in galaxies can at least qualitatively be understood in semi-analytical models of galaxy formation in the framework of hierarchical cosmological build-up of structure[12,15] (see also earlier work of e.g. Eisenstein & Loeb[7]). These studies are complemented on the observational side by strong correlations found between the central black hole mass and global quantities of the surrounding galaxy or galactic bulge (luminosity or mass, and velocity dispersion[8,9]).

Following Begelman, Blandford & Rees[5], the central black holes of two galaxies will ultimately coalesce with strong gravitational radiation emission, after their mother galaxies have merged. During the early stages of the merger, the stellar component will form a nearly spherical system within the short timescale of violent relaxation. After that, the two supermassive black holes move through the stellar component with a velocity similar to the initial relative motion between the two galaxies. From this moment on, both massive bodies will feel dynamical friction from the surrounding stars. This friction leads the black holes to the newly-formed galactic centre, while the frictional force becomes more efficient

with increasing density. Through this process, the black holes must inevitably 'find' each other and form a binary system[21].

After it forms, the bound binary hardens first through dynamical friction. Once the separation of the binary is too small to be further affected by dynamical friction, there are still flybys and resonant scatterings with individual field stars, the latter providing a further hardening source. In an idealized situation, where the binary is at rest, loss-cone stars on orbits subject to a resonant scattering will be depleted and the hardening of the black hole binary would stall, hardening time scales. may become very long, as was noted by[5]. Close, superelastic three-body scatterings between the black hole binary and single stars, however, will generate a strong recoil on the binary, which thus starts a stochastic walk around in the nucleus, and may always find enough interaction partners for further hardening. Direct N-body simulations with high particle numbers are a veru good tool to study this effect quantitatively[23, 33, 13].

We follow the sinking of two massive black holes in a spherical stellar system. The massive particles become bound under the regime of dynamical friction. Once bound, the binary hardens by three body encounters with surrounding stars. Unlike other assumptions the massive system moves inside the core providing an enhanced supply of reaction partners for the hardening. These are the first results from simulations applying a hybrid "self consistent field" (SCF) and direct Aarseth N–body integrator (NBODY6), which synthesises the advantages of the direct force calculation with the efficiency of the field method. The code is aimed for use on parallel architectures and is therefore applicable for collisional N–body integrations with extraordinarily large particle numbers ($> 10^5$). It opens the perspective to simulate the dynamics of globular clusters with realistic collisional relaxation, as well as stellar systems surrounding a supermassive black hole in galactic nuclei.

These problems attract much attention in the astrophysical community[11]. Work on this has been done either by solving the perturbed two and three body problem in simplified models[37, 26] or by N-body simulations[25, 33, 23, 21]. As this shows, the modelling of binary black hole hardening turns out to be extremely challenging, algorithmically and computationally. This work introduces some details of the problem of a sinking black hole binary.

2 Results

To give an example of one of our models, we have followed the shrinking of two black holes of

$$M_\bullet := 1.00015 \cdot 10^7\,\mathrm{M}_\odot, \tag{1}$$

in a galactic nucleus of $M_{\mathrm{tot}} = 10^9\,\mathrm{M}_\odot$, using 65.000 or in some case 128.000 stellar particles in the simulations. So the mean mass of a particle is $\bar{M} = 1.52588 \cdot 10^4\,\mathrm{M}_\odot$. This choice means that every stellar particle with mass M_* represents a compact star cluster with the order of 10^4 particles. The chosen mass for the black hole particle has approximately the same mass as the central black hole of M31[18]. In a typical model, the initial distance between the black holes is 355.39 pc. They become bound after approximately 40 million years. The total simulated time is approximately 190 million years. At the end of the simulation the black holes' distance varies between 1 pc at the apo-center and 0.2 pc at the peri-center. The semi-major axis of the black hole binary at the time it becomes first

bound is 21 pc. For dimensional analysis we can identify the time the binary becomes first bound with the time it has the first critical separation $a_h \approx GM/\sigma^2$[30], where σ is the velocity dispersion of the stellar system outside of the cusp dominated by the black hole, and M is the total mass of the black hole binary. At this stage the dominant interaction process with the stellar system changes from dynamical friction to three-body encounters. The minimum separation of 0.2 pc at the end of our simulation is precise of the order of the second critical separation $a_{\rm crit} \approx 0.012{\rm pc} \cdot M_8^{0.8}$, where M_8 is the black hole mass in units of $10^8{\rm M}_\odot$. At a semi-major axis of the order of $a_{\rm crit}$ quick gravitational radiation merger sets in; $a_{\rm crit}$ is approximately 0.01 ${a_h}$[24], and since the semimajor axis of our black hole binary at the end of the simulation is still 0.6 pc, we are only a fector of three away from the gravitational radiation merger. This is closer than any previously published models of that kind, and similar to the models of Milosavljevic & Merritt[30], who use the same code for the central region than we.

The final eccentricity of the black hole binary in our model varies around 0.7. It depends on the initial eccentricity; we start with more eccentric orbit of the black hole than Milosavljevic & Merritt's models[30], whose black hole binary starts on a circular orbit, and they obtain smaller final eccentricities of only 0.3. This depends on the merging history of the nucleus and its density structure. Eccentricity is of crucial importance for the final fate of the black hole binary since the gravitational radiation time scale becomes much smaller for high eccentricities. The evolution of the orbital data of the black hole binary can be seen in Fig. 1. More details are published in Hemsendorf, Sigurdsson & Spurzem[13].

In total we have performed a number of (up to now) ten different runs used to acquire a small statistical data basis. As one example we show the time evolution of the semi-major axis of the black hole binary in an ensemble averaged sense (error bars are intrinsic 1-σ scatter of the data). We also find a smaller than expected decrease of the motion of the black hole binary's centre of mass with increasing particle number. Despite of expectation that Brownian motion of the black hole binary should decrease with increasing N, we find that our results are consistent with no dependency on particle number. That would mean this effect is not a classical Brownian motion, but other effects, e.g. induced by the superelastic scatterings or collective interactions with the stellar system's core play a role. Our statistical data (compare Figs. 5 and 6 of Hemsendorf, Sigurdsson & Spurzem[13] for the available data on statistically averaged motion of the black hole binary) are not yet complete and reliable enough to give further conclusions here.

This motion prevents the binary from easily evacuating surrounding stars, which establishes an efficient hardening even at the late stages when dynamical friction becomes less important for this. Movies in MPEG format (1.6MB) of this process are available at

`ftp://ftp.ari.uni-heidelberg.de/pub/staff/marc/MPEG/simulation600.mpeg`

This movie (as well as `simulations800.mpeg` and `simulations400.mpeg`) illustrates in the first stages the standard shrinking of the binary black hole to the centre by dynamical friction, then, in the second stages, the feebback effects it has on the core as it moves through the nucleus, and the sometimes rather chaotic motion of the black hole binary, which in our interpretation is responsible for the relatively high eccentricity.

How our present results scale to the case of real particle number of galactic nuclei is the subject of future work. Within the next years and subject to appropriate computing equipment we will be able to follow the black hole binary into its gravitational radiation

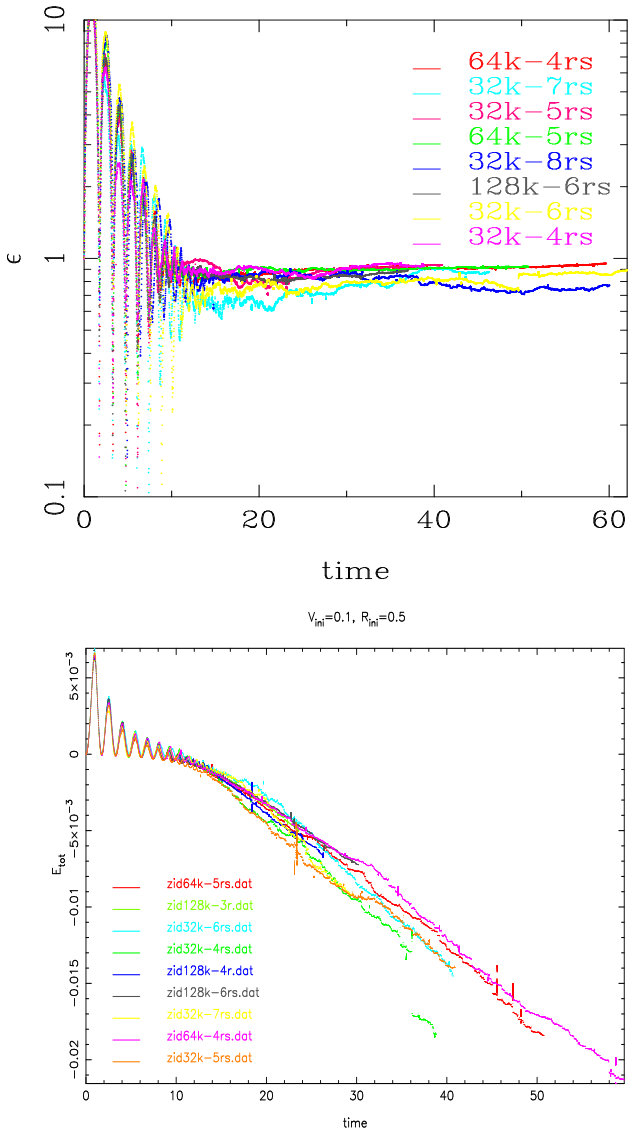

Figure 1. Development of the orbit eccentricity of the black hole binary as a function of time in model time units (top panel) and its binding energy as a function of time, for a sequence of runs with different N, as indicated in the key. Runs denoted with s start with smaller initial eccentricity. Note, that if the binary is not yet bound there are formally values of $a > 0$ and $e > 1$. This means that in that phase the black holes are still not yet gravitationally bound to each other.

merger phase. We have not examined yet the question what happens if a third black hole comes in before the first binary merges. Conventional wisdom says (e.g. Valtonen[38]) that slingshot ejections would eject single or even binary black holes. Recent huge direct N-body models performed by Makino (personal communication) using a GRAPE-6 special purpose computer suggest however, that before that happens, there is a large chance that two black holes in the resonant three-body interaction come very close to each other (eccentricity 0.99) to merge quickly. We have, however, much more carefully than any other study examined the black hole motion in a self-consistent study with very large particle number.

EuroStar proved to be capable of integrating the binary black hole problem in galactic centres as a point mass system. The simulations introduced in this work are the first fully collisional simulations in this field, which could only be carried out on the up-to-date parallel computers accessible to the authors. The new code is going to be applied for simulating collisional dynamics for large N spherical systems including very massive particles.

3 Algorithmic and Computational Aspects

Assume a set of N particles with positions $\vec{r}_i(t_0)$ and velocities $\vec{v}_i(t_0)$ ($i = 1, \ldots, N$) is given at time $t = t_0$, and let us look at a selected test particle at $\vec{r} = \vec{r}_0 = \vec{r}(t_0)$ and $\vec{v} = \vec{v}_0 = \vec{v}(t_0)$. Note that here and in the following the index i for the test particle i and also occasionally the index 0 indicating the time t_0 will be dropped for brevity; sums over j are to be understood to include all j with $j \neq i$, since there should be no self-interaction. Accelerations $\vec{a}_0$ and their time derivatives $\dot{\mathbf{a}}_0$ are calculated explicitly:

$$\vec{a}_0 = \sum_j G m_j \frac{\vec{R}_j}{R_j^3} \;\; ; \;\; \dot{\vec{a}}_0 = \sum_j G m_j \left[\frac{\vec{V}_j}{R_j^3} - \frac{3(\vec{V}_j \cdot \vec{R}_j)\vec{R}_j}{R_j^5} \right] , \tag{2}$$

where $\vec{R}_j := \vec{r} - \vec{r}_j$, $\vec{V}_j := \vec{v} - \vec{v}_j$, $R_j := |\vec{R}_j|$, $V_j := |\vec{V}_j|$. By low order predictions,

$$\begin{aligned} \vec{x}_p(t) &= \frac{1}{6}(t - t_0)^3 \dot{\vec{a}}_0 + \frac{1}{2}(t - t_0)^2 \vec{a}_0 + (t - t_0)\vec{v} + \vec{x} \, , \\ \vec{v}_p(t) &= \frac{1}{2}(t - t_0)^2 \dot{\vec{a}}_0 + (t - t_0)\vec{a}_0 + \vec{v} \, , \end{aligned} \tag{3}$$

new positions and velocities for all particles at $t > t_0$ are calculated and used to determine a new acceleration and its derivative directly according to Eq. 2 at $t = t_1$, denoted by $\vec{a}_1$ and $\dot{\vec{a}}_1$. On the other hand $\vec{a}_1$ and $\dot{\vec{a}}_1$ can also be obtained from a Taylor series using higher derivatives of $\vec{a}$ at $t = t_0$:

$$\begin{aligned} \vec{a}_1 &= \frac{1}{6}(t - t_0)^3 \vec{a}_0^{(3)} + \frac{1}{2}(t - t_0)^2 \vec{a}_0^{(2)} + (t - t_0)\dot{\vec{a}}_0 + \vec{a_0} \, , \\ \dot{\vec{a}}_1 &= \frac{1}{2}(t - t_0)^2 \vec{a}_0^{(3)} + (t - t_0)\vec{a}_0^{(2)} + \dot{\vec{a}}_0 \, . \end{aligned} \tag{4}$$

If $\vec{a}_1$ and $\dot{\vec{a}}_1$ is known from direct summation (from Eq. 2 using the predicted positions and velocities) one can invert the equations above to determine the unknown higher order derivatives of the acceleration at $t = t_0$ for the test particle:

$$\begin{aligned} \frac{1}{2}\vec{a}^{(2)} &= -3\frac{\vec{a}_0 - \vec{a}_1}{(t - t_0)^2} - \frac{2\dot{\vec{a}}_0 + \dot{\vec{a}}_1}{(t - t_0)} \\ \frac{1}{6}\vec{a}^{(3)} &= 2\frac{\vec{a}_0 - \vec{a}_1}{(t - t_0)^3} - \frac{\dot{\vec{a}}_0 + \dot{\vec{a}}_1}{(t - t_0)^2} \, , \end{aligned} \tag{5}$$

This is the Hermite interpolation, which finally allows to correct positions and velocities at t_1 to high order from

$$\begin{aligned} \vec{x}(t) &= \vec{x}_p(t) + \frac{1}{24}(t - t_0)^4 \vec{a}_0^{(2)} + \frac{1}{120}(t - t_0)^5 \vec{a}^{(3)} \, , \\ \vec{v}(t) &= \vec{v}_p(t) + \frac{1}{6}(t - t_0)^3 \vec{a}_0^{(2)} + \frac{1}{24}(t - t_0)^4 \vec{a}_0^{(3)} \, . \end{aligned} \tag{6}$$

Taking the time derivative of Eq. 6 it turns out that the error in the force calculation for this method is $\mathcal{O}(\Delta t^4)$, as opposed to the widely used leap-frog schemes, which have a force error of $\mathcal{O}(\Delta t^2)$. Additional errors induced by approximate potential calculations (particle mesh or TREE) create potentially even larger errors than that. However, it can be shown that the above Hermite method used for a real N-body integration sustains an error of $\mathcal{O}(\Delta t^4)$ for the entire calculation[19]. Many persons in the world know as Aarseth scheme (in particular the code version NBODY5[1]) an integrator of the same order as the Hermite scheme, but using only accelerations on four time points instead of $\vec{a}$ and $\dot{\vec{a}}$ on two time points. As is shown by Makino[19], the Aarseth scheme is $\mathcal{O}(\Delta t^4)$ as well, but for the same number of time steps the absolute value of the energy error (not its slope) is clearly smaller in the Hermite scheme. This means that for a given energy error the Hermite scheme allows timesteps which are larger by some factor of order unity depending on the parameters of the system under study. The Hermite scheme has been commonly adopted during the past years[2], because it needs less memory, and allows slightly larger timesteps. More importantly, after the addition of a hierarchical (as opposed to individual) time step scheme it is well suited for parallelization on modern special and general purpose high performance computers[35]. The timestep scheme will be discussed now.

4 Choice of Timesteps – Parallelization

Aarseth[1] provides an empirical timestep criterion

$$\Delta t = \sqrt{\eta \frac{|\vec{a}||\vec{a}^{(2)}| + |\dot{\vec{a}}|^2}{|\dot{\vec{a}}||\vec{a}^{(3)}| + |\vec{a}^{(2)}|^2}} \; . \tag{7}$$

The error is governed by the choice of η, which in most practical applications is taken to be $\eta = 0.01 - 0.04$. It is instructive to compare this with the inverse square of the curvature κ of the curve $\vec{a}(t)$ in coordinate space

$$\frac{1}{\kappa^2} = \frac{1 + |\dot{\vec{a}}|^2}{|\vec{a}^{(2)}|^2} \; . \tag{8}$$

Clearly under certain conditions the time step choice Eq. 7 becomes similar to choosing the timestep according to the curvature of the acceleration curve; since it was determined just empirically, however, it cannot generally be related to the curvature expression above. Makino[19] suggests a different time step criterion, which appears simpler and more straightforwardly defined, and couples the timestep to the difference between predicted and corrected coordinates. The standard Aarseth time step criterion Eq. 7 has been used in most N-body simulations so far (but compare the discussion by Sweatman[36]).

Since the position of all field particles can be determined at any time by the low-order prediction Eq. 3, the time step of each particle (which determines the time at which the corrector Eq. 6 is applied) can be freely chosen according to the local requirements of the test particle, practically, however, for the purpose of efficient parallelization (originally: vectorization) a hierarchical quantized time step scheme is used, where each particle can only obtain a time step out of a finite set of values[20]. In practice the timestep is taken from the set $\{2^i | i = -n, 0\}$ with $n \leq 32$.

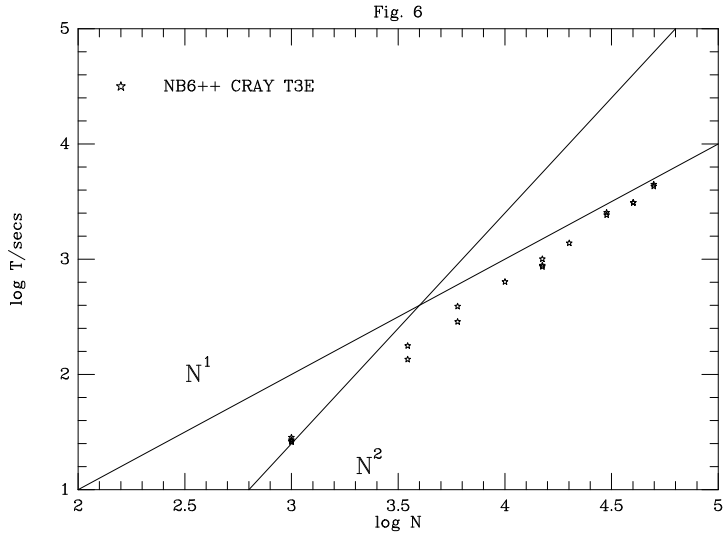

Figure 2. CPU time needed for one N-body time unit as a function of particle number N using NBODY6++ on the CRAY T3E. The collection of data points includes runs with varying average neighbour number and processor/pipeline number, starting from 8 for low N up to 512 for the largest N, which are not individually discriminated in the figure.

Another refinement of the Hermite or Aarseth "brute force" method is the two-time step scheme, denoted as neighbour or Ahmad-Cohen scheme[3]. For each particle a neighbour radius is defined, and $\vec{a}$ and $\vec{\dot{a}}$ are computed due to neighbours and non-neighbours separately. Similar to the Hermite scheme the higher derivatives are computed separately for the neighbour force (irregular force) and non-neighbour force (regular force). Computing two timesteps, an irregular small $\Delta t_{\rm irr}$ and a regular large $\Delta t_{\rm reg}$, from these two force components by Eq. 7 yields a timestep ratio of $\gamma := \Delta t_{\rm reg}/\Delta t_{\rm irr}$ being in a typical range of 5–20 for N of the order 10^3 to 10^4. The reason is that the regular force has much less fluctuations than the irregular force.

If the two-body force between any pair of particles becomes dominant their (perturbed) relative motion is integrated in special regularized coordinates (taking into account perturbations from field particles), in which the singularity of the two-body motion is transformed into a slowly varying parameter (the binding energy) and does not occur in the integration variables. The rest of the N-body simulation generally regards the regularized pair as a compound particle located at the position and moving with the velocity of its centre of mass, except in the case when a perturber moves very close to a regularized pair (in such cases the pair is resolved). An excellent account of regularization, historically and scientifically has been given by Mikkola[27]. Most recent developments are the slow-down treatment of tight binaries[28] and a new method to gain accuracy and exact solutions in the unperturbed case using Stumpff functions[29].

For the binary black hole models of galactic nuclei described in the previous section a hybrid code was used, which embeds the direct N-body region in a larger system, where the potential is approximately computed by a serious evaluation; the latter piece is denoted

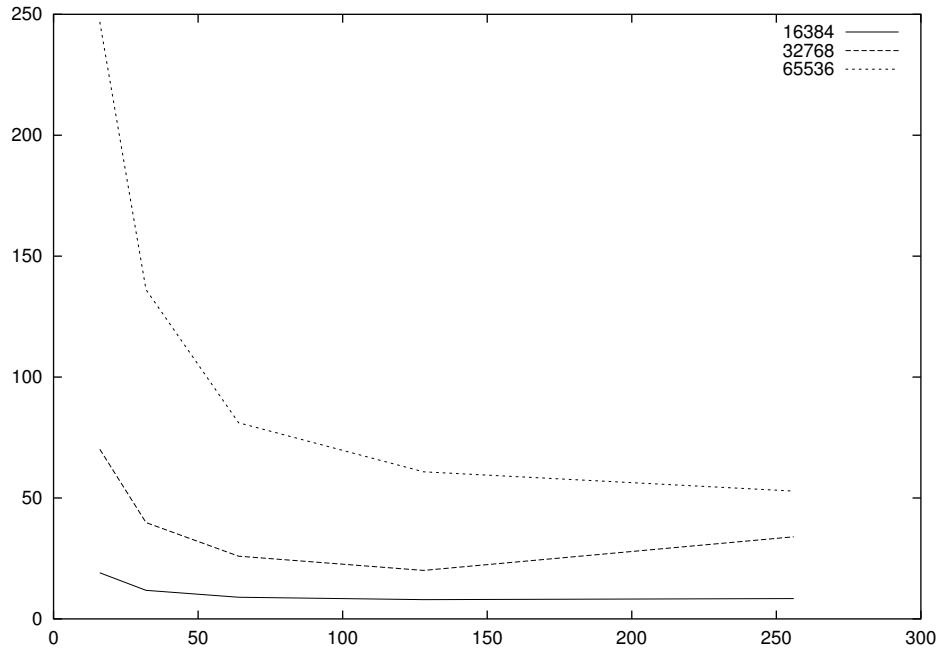

Figure 3. Wall clock time for 200 *SCF* time steps with varying PE number on the *CRAY-T3E*, for the indicated particle numbers. particles, the lower for 16384.

by some authors as SCF ("self-consistent fields"[14]). In Fig. 3 the speed-up of the combined code as a function of the number of nodes is displayed. For parallelization we use a hand-made MPI implementation, parallelizing strategic loops, which need most of the CPU time. The direct N-body portion of the code (particle-particle interactions) is the most dominant one still, and it uses a parallel force computation for the long-range and short-range forces in a loop over those particles which are due for integration in the individually blocked time step scheme. No domain decomposition is used here yet, all particle data are sent in copy to all PE's. Here, a typical integration time needed is about 1 hour wall clock for 128k particles on 128 processors of the CRAY T3E. A model for the binary black hole problem requires for each individual run about 60 time units. Models for the globular star clusters are much more complicated, because they need a few hundred time units in physical time (long relaxation time). Also regularized binaries are present in a larger number, and there are physical hints from star formation that we should include in our models thousands of close binaries from the very beginning[10]. Future work on improvement of our implementation is therefore directed in two directions: first an efficient parallel integration of the regularized pairs (work nearly completed now with S.J. Aarseth), and second, a domain decomposition and division of the force for the very distant particles, in order not to lose accuracy but gain efficiency. The recent papers of Makino[22] and Dorband, Hemsendorf & Merritt[6] both discuss future prospects regarding the use of hypersystolic algorithms and non-blocking communication.

Acknowledgements

The authors would like to thank S. Aarseth and D. Merritt for fruitful help and discussion. This project is funded by Sonderforschungsbereich (SFB) 439 “Galaxies in the Young Universe” at the University of Heidelberg. Support and computer resources awarded by *NIC* Jülich and *HLRS* in Stuttgart are gratefully acknowledged.

References

1. Aarseth, S.J. 1985, in Brackbill J.U., Cohen B.I., eds, Multiple time scales, Academic Press, Orlando, 378.
2. Aarseth, S.J., 1999, CeMDA 73, 127.
3. Ahmad, A., Cohen, L., 1973, Journ. Comp. Phys., 12, 389.
4. Amaro-Seoane, P., Spurzem, R., 2001, MNRAS, 327, 995.
5. Begelman, M.C., Blandford, R.D., & Rees, M.J., 1980, Nature, 287, 307.
6. Dorband N., Hemsendorf M., Merritt D., 2001, Thesis Rutgers Univ., astro-ph/0112092.
7. Eisenstein, D.J., Loeb, A., 1995, ApJ, 448, 17L.
8. Ferrarese, L., Merritt, D. 2000, ApJ, 539, L9.
9. Gebhardt, K., Richstone, D., Kormendy, J., Lauer, T.R., Ajhar, E.A., Bender, R., Dressler, A., Faber, S.M., Grillmair, C., Magorrian, J., Tremaine, S., 2000, AJ, 119, 1157.
10. Giersz, M., Spurzem, R., 2000, MNRAS, 317, 581.
11. Gould, A., Rix, H.W., 2000, ApJ, 532, L29.
12. Haehnelt, M., Kauffmann, G. 2000, MNRAS, 318, 35L.
13. Hemsendorf, M., Sigurdsson, S., Spurzem, R., 2001, subm. ApJ, astro-ph/0103410.
14. Hernquist, L., Ostriker, J.P., 1992, ApJ, 386, 375.
15. Kauffmann, G., Haehnelt, M. 2000, MNRAS, 311, 576.
16. Kormendy, J., Richstoner, D., 1995, ARA&A, 33, 581.
17. Langbein, T., Spurzem, R., Fricke, K.J., Yorke, H.W., 1990, A&A, 227, 333.
18. Magorrian, J., *et al.*, 1998, AJ, 115, 2285.
19. Makino, J., 1991a, ApJ, 369, 200.
20. Makino, J., 1991b, PASJ, 43, 859.
21. Makino, J., 1997, ApJ, 478, 58.
22. Makino J., 2001, subm. New Astronomy, astro-ph/0108412.
23. Makino, J., Fukushige, T., Okumura, S.K., Ebisuzaki, T., 1993, PASJ, 45, 303.
24. Merritt, D., 2001, ApJ, 556, 245.
25. Merritt, D., Quinlan, G.D., 1998, ApJ, 498, 625.
26. Mikkola, S., Valtonen, M.J., 1992, MNRAS, 259, 115.
27. Mikkola, S., 1997, CeMDA, 68, 87.
28. Mikkola, S., Aarseth, S. J., 1996, CeMDA, 64, 197.
29. Mikkola, S., Aarseth, S. J., 1998, NewA, 3, 309.
30. Milosavljevic, M., Merritt, D., 2001, subm. ApJ, astro-ph/0103350.
31. Peebles, P.J.E. 1993, *Principles of physical cosmology*, Princeton : Princeton University Press.
32. Quinlan, G.D., Shapiro, S.L., 1990, ApJ, 356, 483.

33. Quinlan, G.D., Hernquist, L., 1997, NewA, 2, 533.
34. Spurzem, R., Baumgardt, H. 2001, submitted to Monthly Notices of the Royal Astronomical Society (`ftp://ftp.ari.uni-heidelberg.de/pub/staff/spurzem/edinpaper.ps.gz`).
35. Spurzem, R., 1999, in Riffert, H., Werner, K. (eds), Computational Astrophysics, The Journal of Computational and Applied Mathematics (JCAM) 109, Elsevier Press, Amsterdam, 407.
36. Sweatman, W. L., 1994, Journ. Comp. Phys., 111, 110.
37. Valtonen, M.J., Mikkola, S., Heinämäki, P., Valtonen, H., 1994, ApJS, 95, 69.
38. Valtonen, M. J., 1996, MNRAS 278, 186.